VNU Journal of Science: Mathematics – Physics, Vol. 33, No. 1 (2017) 14-21

Synthesis, Magnetic Properties and Enhanced Photoluminescence of Fe_3O_4-ZnO Heterostructure Multifunctional Nanoparticles

Chu Tien Dung[1,2], Luu Manh Quynh[1], Tran Thi Hong[3], Nguyen Hoang Nam[1,*]

[1]*Faculty of Physics, VNU University of Science, 334 Nguyen Trai, Thanh Xuan, Hanoi, Vietnam*
[2]*Department of Physics, University of Transport and Communications, 3 Cau Giay, Hanoi, Vietnam*
[3]*VNU University of Science, 334 Nguyen Trai, Thanh Xuan, Hanoi, Vietnam*

Received 10 January 2017
Revised 25 February 2017; Accepted 20 March 2017

Abstract: In this paper, Fe_3O_4-ZnO heterostructure multifunctional nanoparticles (NPs) were successfully prepared in aqueous solution by ultrasound assisted thermolysis. First, iron oxide (Fe_3O_4) magnetic NPs were prepared by co-precipitation method. The Fe_3O_4 NPs were modified by 3-aminopropyltriethoxysilane (APTES) to have free amine (-NH_2) groups on their surface, then, Zn^{2+} ions were added and stirred to adsorb onto the surface of Fe_3O_4-NH_2 NPs in alkaline solution at a pH of 11. This solution was decomposed through thermolysis in ultrasound bath. The results of measurements show that photoluminescence of Fe_3O_4-ZnO heterostructure multifunctional NPs was enhanced in visible light at 565 nm wavelength to allow detection, labeling, diagnosis, and therapy in biomedicine. Moreover, they exhibit superparamagnetic properties of Fe_3O_4 with high saturation magnetization (M_S), which can be used for seperation application in biomedicine under an external magnetic field.

Keywords: Fe_3O_4-ZnO, multifunctional nanoparticles, heterostructure, enhanced photoluminescence.

1. Introduction

In recent years, multifunctional nanoparticles (MNPs) based on fluorescent, magnetic, and plamonic nano-materials are becoming very important materials, which have been a hot research field in material sciences. Among these MNPs, the NPs combining luminescent and magnetic are the most popular because of their wide variety of applications in magnetic resonance imaging (MRI), targeted drug delivery, separation, biodetection, and photodynamic therapy [1-4].

For the magnetic obligation, Fe_3O_4 NPs are one of the most studied popular materials, are due to not only their novel properties such as superparamagnetism but also for their potential applications such as MRI constrast agent [1], separation [2], and hyperthermia therapy to targeted delivery [3],.

*Corresponding author. Tel.: 84-913020286
Email: namnh@hus.edu.vn

Furthermore, quantum dots (QDs) are particularly attractive for the luminescent properties because of their tunable emission peak, high photoluminescence quantum yield, and remarkable photostability [5-7]. The QDs are ideal materials for using as luminescent probes for bioapplications [2-4,8-10]. Among these QDs, zinc oxide (ZnO) NPs emerge with unique physical and chemical properties such as high chemical stability, high photoluminescence, bio-compatibility, and nontoxicity [5,8,9]. Therefore, it would be significant to combine the Fe_3O_4 NPs with the QDs to form the MNPs with potential applications for detecting, labeling, and separating biological entities by using luminescence imaging method under an external magnetic field [4]. Nowadays, the MNPs such as Fe_2O_3-CdS, Fe_3O_4-CdS have synthesized extensively [11, 12]. Although these magnetic-optical materials have disadvantage due to unbiocompability, toxicity of the QDs (CdSe, CdS), and complicated synthesis protocol [6,13].

Herein, we have synthesized Fe_3O_4-ZnO heterostructure MNPs in aqueous solution by ultrasound assisted thermolysis and investigated their characterizations. It is promised that the MNPs are an ideal system for bioapplications because of their superparamagnetic feature and enhancing luminescent properties.

2. Experimental

The Fe_3O_4 was synthesized by co-precipitation method using Fe^{2+}/Fe^{3+} with 1:2 molar ratios from the two chloride salts of $FeCl_2$ and $FeCl_3$, was evenly dispersed in ethanol according to our research [14].

10.5 mg Fe_3O_4 was equally dispersed in 20 ml ethanol by ultrasound waves, before 5.5 ml ammonia solution 28% and 4.5 ml aminopropyltriethoxysilane $H_2N(CH_2)_3Si(OC_2H_5)_3$ (APTES) were added and vibrated in ultrasound bath with keeping stable temperature at 45^oC to form $–O–Si–(CH_2)_3–NH_2$ group onto the surface of the Fe_3O_4 NPs [15]. The solution is then washed several times with ethanol to collect $Fe_3O_4–NH_2$.

The $Fe_3O_4–NH_2$ were dispersed in 20 ml ethanol by ultrasound waves before ammonia solution 28% was added to have solution at a pH of 11. Then, 1ml ion Zinc (Zn^{2+}) 0.2 M was injected and stirred to adsorb onto the surface of the Fe_3O_4-NH_2. Finally, this solution was decomposed through thermolysis in ultrasound bath for 2h. The Fe_3O_4-ZnO NPs were collected after washing several times with ethanol and distilled water.

ZnO NPs was synthesized at the same condition with the Fe_3O_4-ZnO sample. As, 1ml ion Zinc (Zn^{2+}) 0.2 M was injected, stirred in 20 ml Ethanol at a pH of 11, was then decomposed through thermolysis in ultrasound bath for 2h. The ZnO NPs were collected after washing several times with ethanol and distilled water.

The crystalline structure was observed by x-ray diffraction (XRD), recorded by using a SIEMENS D5005 (Bruker-Germany) diffractometer. To study the formation of chemical bonds in the Fe_3O_4, $Fe_3O_4–NH_2$, ZnO and Fe_3O_4-ZnO NPs, Fourier transform infrared (FTIR) spectroscopy measurement was carried out on 8400S Shimadzu-Japan. Sample qualitative and quantitative compositions were investigated by using energy dispersive x-ray *spectroscopy (EDS), obtained with ISIS 300 system (Oxford - UK).* The size and morphology of the Fe_3O_4 and Fe_3O_4-ZnO were investigated by a JEOL JEM-1010 transmission electron microscope (TEM), which was operated at 80 kV. *The magnetic hysteresis loops of samples were characterised by* vibrating sample magnetometer *(VSM) on Digital Measurement Systems 880 (from USA). Photoluminescence (PL) spectra were recorded by using an* Fluorolog FL3-22 (Jobin-Yvon-Spex, USA) *spectrophotometer.*

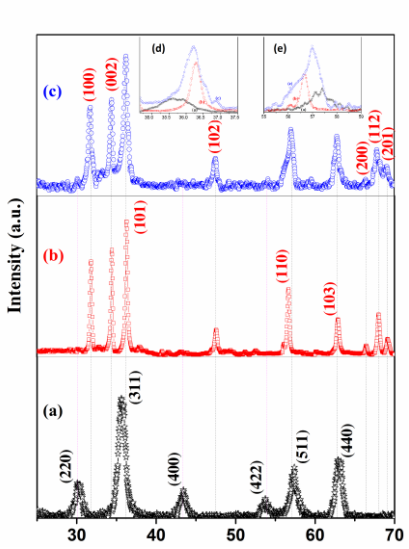

Figure 1. XRD of Fe_3O_4 (a); ZnO (b); Fe_3O_4-ZnO (c); insets show zoom-in overlap spectra of all samples at 34.6^o-37.5^o (d) and 55^o-59^o (e).

3. Results and discussion

The phase and crystallinity of the as-prepared samples were shown in Figure 1. In the Figure 1(a) shows the XRD patterns of the Fe_3O_4. Six diffraction peaks observed at 30.03^o, 35.49^o, 43.35^o, 53.55^o, 57.39^o, 62.87^o, marked by their Miller indices (220), (311), (400), (422), (511), and (440) respectively. They can be well indexed to the face centered cubic spinel structure of the Fe_3O_4 in JCPDS cards No. 19-0629. Average lattice parameter of the Fe_3O_4 crystal was calculated as $\bar{a} = 8.36$ Å, which is in agreement with published results [16]. Average crystalline size of the Fe_3O_4 was calculated as $\bar{D} = 7.8 \pm 2.7\ (nm)$ from the full width at half maximum (FWHM) of the most intense diffraction peaks by using the Debye-Scherrer equation [16]. In the Figure 1(b), the peaks located at $2\theta = 31.83^o$, 34.47^o, 36.32^o, 47.57^o, 56.68^o, 62.91^o, 66.45^o, 68.01^o, and 69.13^o were respectively indexed to the (100), (002), (101), (102), (110), (103), (200), (112), and (201) diffraction planes of ZnO crystals with a hexagonal wurtzite structure when compared to the standard diffraction in JCPDS cards No. 36-1451. The average lattice parameter of the ZnO is calculated as $\bar{a} = 3.25$ Å and $\bar{c} = 5.21$ Å, which are consistent with reported papers [5,9,10]. The XRD patterns of the Fe_3O_4-ZnO MNPs in the Figure 1(c) shows that it has discernible diffraction peaks locating at 31.81^o, 34.47^o, 36.14^o, 47.53^o, 57.02^o, 62.84^o, 67.95^o, and 69.09^o, were indexed to diffraction planes of the ZnO. In the Figure 1(c) exposes very low diffraction peaks locating at 30.07^o and 53.64^o, were indexed to diffraction planes of the Fe_3O_4. Moreover, the diffraction peaks of the Fe_3O_4-ZnO were broaden to cover simultaneously diffraction peaks of the Fe_3O_4 and the ZnO. In the Figure 1(d-e), insets show zoom-in overlap spectra of the Fe_3O_4, ZnO, and the Fe_3O_4-ZnO at 34.6^o-37.5^o, and 55^o- 59^o, respectively, indicating that the MNPs compose of crystallite the Fe_3O_4 and the ZnO. Herein, the ZnO NPs is deposited onto the surface of the Fe_3O_4-NH_2 to form shell layer covering the Fe_3O_4 core, which hinders x-rays from penetrating deeper into the Fe_3O_4-ZnO NPs. Hence, a direct observation of the Fe_3O_4 phases cannot be clearly seen [17].

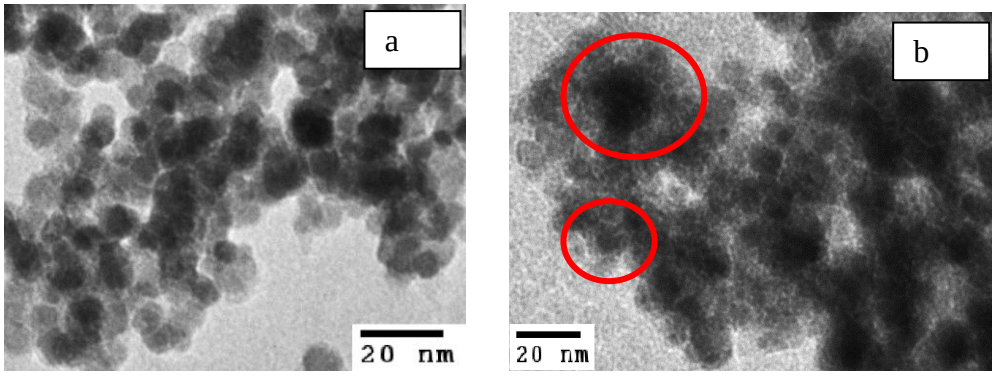

Figure 2. TEM image of Fe_3O_4 (a); Fe_3O_4-ZnO (b)

Figure 2(a) is a TEM image of the as-prepared Fe_3O_4 NPs. It reveals almost homogeneous, relatively spherical shape and a diameter of 6 nm to 14 nm, which is consistent with calculation from XRD patterns for the diameter of the Fe_3O_4 NPs. The TEM image of the Fe_3O_4-ZnO MNPs in Figure 2(b) shows that in red circles, it can be seen two parts: interior part is high contrast, which may be the Fe_3O_4 modified by APTES; exterior part is lower contrast, which may be the ZnO nanocrystals. Agglomeration of the Fe_3O_4-ZnO as presented in Figure 2(b) can be due to modification of the Fe_3O_4 NPs with APTES and the existence of small remanence magnetization of the Fe_3O_4 [15].

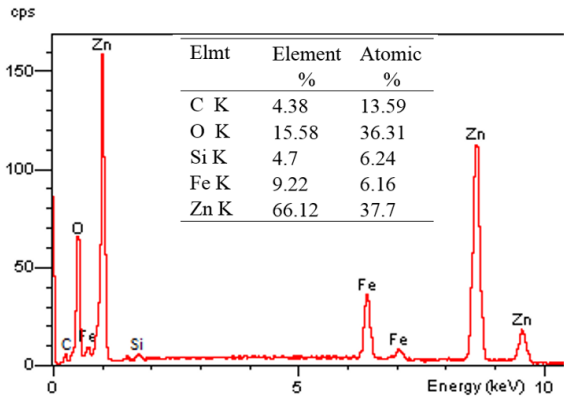

Elmt	Element %	Atomic %
C K	4.38	13.59
O K	15.58	36.31
Si K	4.7	6.24
Fe K	9.22	6.16
Zn K	66.12	37.7

Figure 3. Energy dispersive x-ray *spectro-scopy* of Fe_3O_4-ZnO and insert table of percent of elements composition.

Figure 3 displays energy dispersive X-ray *spectroscopy of the* Fe_3O_4-ZnO MNPs and insert a table of percent of elements composition. The presence of Fe and Zn determines that the MNPs are simultaneously composed of the Fe_3O_4, ZnO nanocrystals. Furthermore, the existence of C and Si provide direct proof for the successful modification of APTES on the surface of the Fe_3O_4 NPs.

Figure 4(left) shows FTIR spectra of the Fe_3O_4, Fe_3O_4-NH_2, ZnO and Fe_3O_4-ZnO samples. It can be seen that in the Fe_3O_4, Fe_3O_4-NH_2, and Fe_3O_4-ZnO samples have absorption peaks aroud 425 cm^{-1}, 628 cm^{-1} corresponding to the Fe-O vibration of the Fe_3O_4 phase [18]. Peak at 628 cm^{-1} has shifted to 650 cm^{-1} in the Fe_3O_4-NH_2 samples, which is clear evidence to prove the successful modification of APTES on the surface of the Fe_3O_4, and agrees well with the result from the EDS [19].

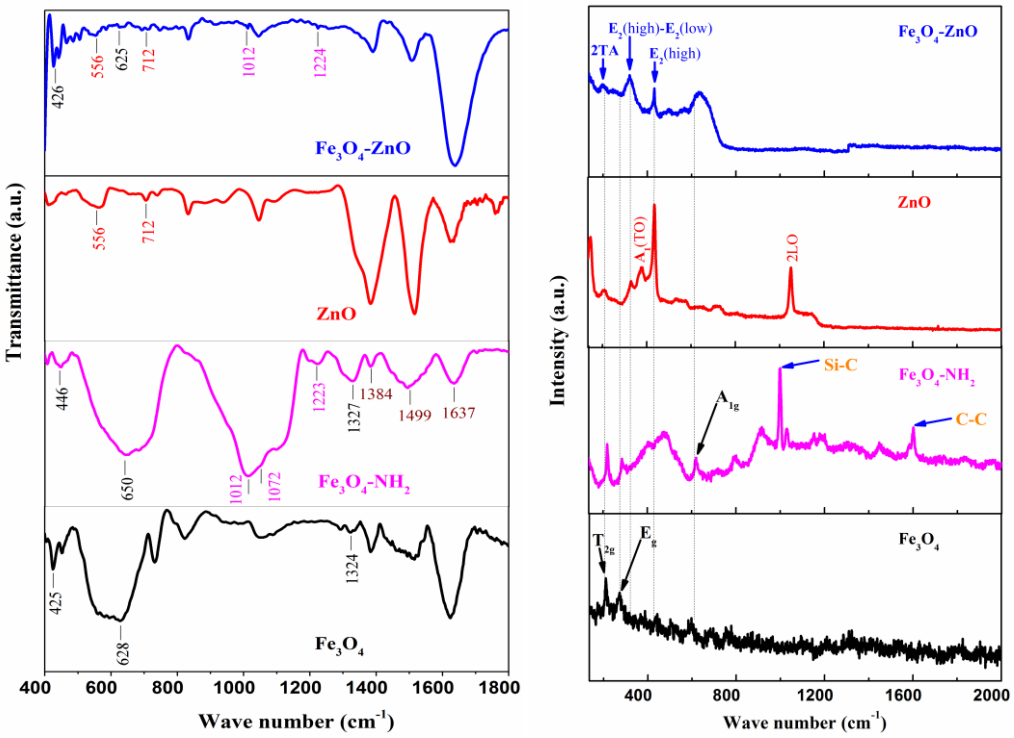

Figure 4. FTIR (left) and Raman shift (right) spectra of Fe_3O_4; Fe_3O_4-NH_2; ZnO and Fe_3O_4-ZnO.

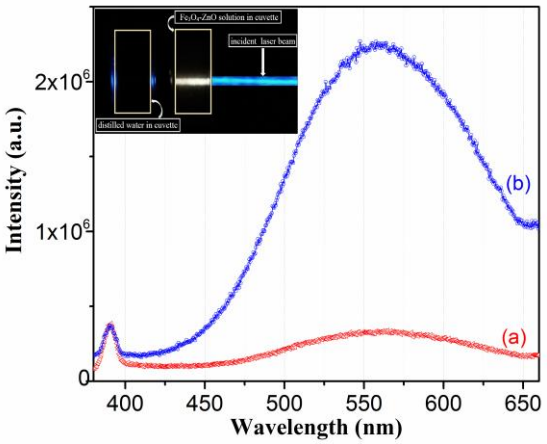

Figure 5. Photoluminesences spectra of ZnO (a); Fe_3O_4-ZnO (b) and inset shows luminescence image using excited laser beam 325 nm wavelength.

Further, the band at 1012 cm^{-1} and 1223 cm^{-1} only observed in the Fe_3O_4-NH_2, are assigned to stretching vibrations of Si-O-Si [15, 19] and vibration of $–CH_2$ [18]. And shoulder at 1072 cm^{-1} is corresponding to stretching vibrations of C-N, which is relating to the $–(CH_2)_3–NH_2$ group onto the

surface of the Fe_3O_4. The peaks at 1384 cm^{-1} are because of the existence of CO_2 molecule in air [20]. The peaks, observed between 1450 cm^{-1} and 1700 cm^{-1}, are allotted the crucial stretching mode of OH [18]. These vibrations indicate the presence of H_2O molecules on the surface of the all samples. On the other hand, the band at 556 cm^{-1} and 712 cm^{-1} is only observed in the ZnO and Fe_3O_4-ZnO samples, can be attributed to the Zn-O stretching mode in the ZnO lattice [20,21]. Interestingly, the peak of the Fe-O vibration in the Fe_3O_4-ZnO MNPs has lower absorption intensity than in the Fe_3O_4 and the Fe_3O_4-NH_2, which indicates that ZnO nanocrystals are assembled onto the surface of the Fe_3O_4-NH_2. Combining with XRD results, it is concluded that the as-prepared Fe_3O_4-ZnO MNPs have core-shell structure.

Raman spectroscopy is useful to probe the local structure. Figure 4(right) presents the Raman spectra of all samples. The sharp peak at 204 cm^{-1}, 287 cm^{-1}, and 611 cm^{-1}, only observed in the Fe_3O_4 and the Fe_3O_4-NH_2 samples, are characterization of the T_{2g}, E_g, and A_{1g} modes of the Fe_3O_4 [22]. The intense Raman shift peaks at 998 cm^{-1} and 1601 cm^{-1} in the Fe_3O_4-NH_2 sample are corresponding to vibration of Si-C [23] and C-C [24], allowing to determine the existence of $–O–Si–(CH_2)_3–NH_2$ group onto the surface of the Fe_3O_4 NPs, which is suitable to the results of FTIR. Raman shift spectrum of the Fe_3O_4-ZnO MNPs shows that the intense and sharp peaks at 332 cm^{-1} and 438 cm^{-1} are characterization of the E_2(high) - E_2(low) and E_2(high) modes of the hexagonal ZnO crystalline structure, which are agreement with that of the ZnO sample [25, 26]. The high frequency E_2(high) mode involves the vibration of oxygen atoms, which is attributed to low intrinsic defects only associated with oxygen such as oxygen vacancies (V_O). In addition, the stronger intensity of the E_2(high) peak is the better quality crystals [25, 26]. The low peak observed at 207 cm^{-1}, is assigned to the 2TA mode of the ZnO nanocrystals and is the agreement with T_{2g} mode in the Fe_3O_4 [26]. These results indicate that ZnO nanocrystals coat surrounding of the Fe_3O_4 NPs, which is consistent with the results of XRD and FTIR.

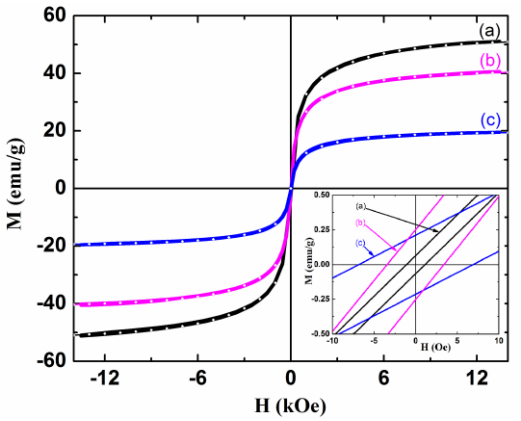

Figure 6. The magnetic hysteresis loops of Fe_3O_4 (a); Fe_3O_4-NH_2 (b) and Fe_3O_4-ZnO (c) at room temperature.

Figure 6 presents the room temperature PL spectra of the ZnO NPs and the Fe_3O_4-ZnO MNPs. The PL spectra shows a broad emission spectrum covering from near ultraviolet to whole of the visible region. All the samples show a small ultraviolet emission peak at approximately 387 nm (equivalent to 3.2 eV), which can be attributed to the near band edge transitions in the ZnO nanocrystals, originating from the recombination of free exciton through an exciton-exciton collision process [27]. Whereas the visible band emission is known to be due to an electronic transition from the conduction band edge to a defect of associated trap state such as an oxygen vacancy, which is consistent with the appearance of E_2(high) mode in Raman shift spectra [28, 29]. Nevertheless, intensity of visible band emission in the

Fe_3O_4-ZnO MNPs was enhanced and was higher than that of the ZnO many times. It can be explained that the formation of core-shell structure of the Fe_3O_4-ZnO MNPs makes trap states, as suggesting valence band and conduction band of the Fe_3O_4 core [26]. So, the center of visible band emission at 565 nm (equivalent to 2.21 eV) in the Fe_3O_4-ZnO MNPs is attributed to can be due to an electronic transition from the conduction band edge of the ZnO nanocrystal to the trap states such as conduction band edge of the Fe_3O_4 core. With high photoluminescence in visible light, the Fe_3O_4-ZnO MNPs are promised application for biosensor [10,26], bioimaging [8,9].

The magnetic hysteresis loops of the Fe_3O_4, Fe_3O_4-NH_2, and the Fe_3O_4-ZnO were measured at room temperature, were displayed in Figure 6. The M_S of the Fe_3O_4, Fe_3O_4-NH_2, and the Fe_3O_4-ZnO have value as 51.8, 40.9, and 19.6 (emu/g), respectively. The decrease of the M_S values can be explained by the successful modification of the APTES on the surface of the Fe_3O_4 NPs and the formation of ZnO nanocrystals surrounding the Fe_3O_4-NH_2. This results can be comfirmed that the MNPs contain simultaneously the Fe_3O_4 and the ZnO nanocrystals. In the Figure 6 shows that the Fe_3O_4, Fe_3O_4-NH_2, and the Fe_3O_4-ZnO are superparamagnetic at room temperature with high M_S and small coercivity (approximately 7 Oe). The magnetic properties results in that the MNPs can be tagged and separated with biomolecules or targeted drug delivery and magnetic resonance imaging (MRI) under the induction of an external magnetic field [3,16].

4. Conclusion

In this paper, the Fe_3O_4-ZnO MNPs were successfully synthesized in aqueous solution by ultrasound assisted thermolysis. The MNPs compose of the magnetic Fe_3O_4 NPs and the photoluminescent ZnO nanocrystals. Moreover, the MNPs not only enhance PL in visible light but also exhibit superparamagnetism with high saturation magnetization at room temperature. These MNPs can make wide variety of applications for biomedical.

Acknowledgements

This study was accomplished at the Center for Material Sciences, VNU University of Sciences. The first author thanks the project 911 - Vietnam education fellowship for financial support.

References

[1] Y.D. Jin, C.X Jia, S.W Huang, M.O. Donnell, and X.H. Gao, "Multifunctional nanoparticles as coupled contrast agents". Nature Communications 1, (2010) 41.

[2] G G. Liu, D. Hu, M. Chen, C.C. Wang, and L.M. Wu, "Multifunctional PNIPAM/Fe_3O_4–ZnS hybrid hollow spheres: Synthesis, characterization, and properties". Journal of Colloid and Interface Science 397 (2013) 73.

[3] H.H. Yiu, "Engineering the multifunctional surface on the magnetic nanoparticles for targeted biomedical applications", Nanomedicine. 6(8) (2011) 1429.

[4] L.W. Chan, Y.N. Wang, L.Y. Lin, M.P. Upton, J.H. Hwang, and S.H. Pun, "Synthesis and Characterization of Anti-EGFR Fluorescent Nanoparticles for Optical Molecular Imaging", Bioconjugate Chem. 24 (2013) 167.

[5] S.T. Dutta, S. Chattopadhyay, A. Sarkar, M. Chakrabarti, D. Sanyal, and D. Jana, "Role of defects in tailoring structural, electrical and optical properties of ZnO", Progress in Materials Science, 54 (2009) 89.

[6] K. Yu, B. Zaman, S. Romanova, D.S.Wang, and J.A. Ripmeester "Sequential Synthesis of Type II Colloidal CdTe/CdSe Core–Shell Nanocrystals", small, 1, No. 3 (2005), 332.

[7] D.A. Bussian, S.A. Crooker, M. Yin, M.Brynda, A.L. Efros, and V.I. Klimov, "Tunable magnetic exchange interactions in manganese-doped inverted core–shell ZnSe–CdSe nanocrystals". Nature materials, 8 (2009) 35

[8] K. Senthilkumar, O. Senthilkumar, K. Yamauchi, M. Sato, S. Morito, T. Ohba, M. Nakamura, and Y. Fujita, "Preparation of ZnO nanoparticles for bio-imaging applications", Phys. Status Solid b, 246 (2009) 885.

[9] J.W. Rasmussen, E. Martinez, P. Louka, and D.G. Wingett, "Zinc Oxide Nanoparticles for Selective Destruction of Tumor cells and Potential for Drug delivery Applications", Expert Opin Drug Deliv, 7 (2010) 1063.

[10] Z.W.Zhao, W. Lei, X.B. Zhang, B.P. Wang, and H.L. Jiang, "ZnO-Based Amperometric Enzyme Biosensors", Sensors. 10 (2010) 1216.

[11] Z. Wu, H. Yu, L. Kuai, H. Wang, T.H. Pei, and B.Y. Geng, "CdS urchin-like microspheres/a-Fe_2O_3 and CdS/Fe_3O_4 nanoparticles heterostructures with improved photocatalytic recycled activities. Journal of Colloid and Interface Science 426 (2014) 83.

[12] A. Roychowdhury, S.P. Pati, S. Kumar, and D. Das, "Tunable properties of magneto-optical Fe_3O_4/CdS nanocomposites on size variation of the magnetic component", Materials Chemistry and Physics, 151 (2015) 105.

[13] S.A.O. Gomes, C.S. Vieira, D.B. Almeida, J.R. Santos-Mallet, R.F. S. Menna-Barreto, C.L. Cesar, and D. Feder, "CdTe and CdSe Quantum Dots Cytotoxicity: A Comparative Study on Microorganisms". Sensors, 11 (2011), 11664.

[14] C.T. Dung, L.M. Quynh, N.P. Linh, N.H. Nam, N.H. Luong, "Synthesis of ZnS:Mn-Fe_3O_4 bifunctional nanoparticles by inverse microemulsion method", Journal of Science: Advanced Materials and Devices 1 (2016) 200.

[15] M. Mahdavi, M.B. Ahmad, M.J. Haron, Y. Gharayebi, K. Shameli, and B. Nadi, "Fabrication and Characterization of SiO_2/(3-Aminopropyl) triethoxysilane-Coated Magnetite Nanoparticles for Lead(II) Removal from Aqueous Solution", J Inorg Organomet Polym, 23 (2013) 599.

[16] H.E. Ghandoor, H.M. Zidan, M.M.H. Khalil, and M.I.M. Ismai, "Synthesis and Some Physical Properties of Magnetite (Fe_3O_4) Nanoparticles". Int. J. Electrochem. Sci., 7 (2012) 5734.

[17] M. Stefan, O. Pana, C. Leostean, C. Bele, D. Silipas, M. Senila, and E. Gautron, "Synthesis and characterization of Fe_3O_4–TiO_2 core-shell nanoparticles". Journal of Applied Physics 116 (2014) 114312.

[18] Y.S. Li, J.S. Church, A.L. Woodhead, and F. Moussa. "Preparation and characterization of silica coated iron oxide magnetic nano-particles". Spectrochimica Acta Part A 76 (2010) 484.

[19] Z. Hassannejad, M.E. Khosroshahi, and M. Firouzi, "Fabrication and Characterization of Magnetoplasmonic Liposome Carriers". Journal of Inorganic and Organometallic Polymers and Materials, 23, 3, (2013) 599.

[20] S. Senthilkumaar, K. Rajendran, S. Banerje, T.K. Chini, and V. Sengodan. "Influence of Mn doping on the microstructure and optical property of ZnO". Mater. Sci. Semicon. Process. 11 (2008) 6.

[21] P. Patra, S. Mitra, N. Debnath, P. Pramanik, and A. Goswami, "Ciprofloxacin conjugated zinc oxide nanoparticle: A camouflage towards multidrug resistant bacteria". Bull. Mater. Sci., 37 (2014) 199.

[22] O.N. Shebanova and P. Lazor. "Raman spectroscopic study of magnetite ($FeFe_2O_4$): a new assignment for the vibrational spectrum". Journal of Solid State Chemistry 174 (2003) 424.

[23] X.X. Qi, G.M. Zhai, J. Liang, S.F. Ma, X.G. Liu, and B.S. Xu. "Preparation and characterization of SiC@CNT coaxial nanocables using CNT as template". CrystEngComm, 16 (2014), 9697.

[24] E.B. Santos, F.A. Sigoli, and I.O. Mazali. "Facile synthesis of the dendritic structure of silver nanoparticles-chitosan and its application as an effective SERS substrate". New J. Chem. 38 (2014) 5369.

[25] Y.Q. Huang, M.D. Liu, Z. Li, Y. Zeng, and S.B. Liu, "Raman spectroscopy study of ZnO-based ceramic films fabricated by novel sol gel process". Materials Science and Engineering B 97 (2003) 111.

[26] C.Karunakaran and P. Vinayagamoorthy. "Magnetically recoverable Fe3O4-implanted Ag-loaded ZnO nanoflakes for bacteria-inactivation and photocatalytic degradation of organic pollutants". New J. Chem., 40 (2016) 1845.

[27] Z.K. Tang, M. Kawasaki, A. Ohtomo, H. Koinuma, and Y. Segawa, "Self-assembled ZnO nano-crystals and exciton lasing at room temperature". Journal of Crystal Growth, 287 (2006) 169.

[28] N.S. Norberg, and D.R. Gamelin. "Influence of Surface Modification on the Luminescence of Colloidal ZnO Nanocrystals". J.Phys.Chem B, 109 (2005) 20810.

[29] K. Vanheusden, W.L. Warren, C.H. Seager, D.R. Tallant, and J.A. Voigt, "Mechanisms behind green photoluminescence in ZnO phosphor powders". Journal of Applied Physics, 79 (1996) 7983.